

1-1-2007

Deformation-induced nanoscale high-temperature phase separation in Co-Fe alloys at room temperature

Laichang Zhang
IFW Dresden, laichang@uow.edu.au

M Calin
IFW Dresden

F Paturaud
IFW Dresden

C Mickel
IFW Dresden

J Eckert
IFW Dresden

Follow this and additional works at: <https://ro.uow.edu.au/engpapers>



Part of the [Engineering Commons](#)

<https://ro.uow.edu.au/engpapers/3572>

Recommended Citation

Zhang, Laichang; Calin, M; Paturaud, F; Mickel, C; and Eckert, J: Deformation-induced nanoscale high-temperature phase separation in Co-Fe alloys at room temperature 2007, 201908-1-201908-3.
<https://ro.uow.edu.au/engpapers/3572>

Deformation-induced nanoscale high-temperature phase separation in Co–Fe alloys at room temperature

Lai-Chang Zhang^{a)}*IFW Dresden, Institut für Komplexe Materialien, Postfach 27 01 16, D-01171 Dresden, Germany*

Mariana Calin

IFW Dresden, Institut für Komplexe Materialien, Postfach 27 01 16, D-01171 Dresden, Germany and Materials Science and Engineering Faculty, University Politehnica of Bucharest, Spl. Independentei 313, R-060032 Bucharest, Romania

Flora Paturaud

W.C. Heraeus GmbH, Heraeusstr. 12-14, D-63450 Hanau, Germany

Christine Mickel

IFW Dresden, Institut für Metallische Werkstoffe, Postfach 27 01 16, D-01171 Dresden, Germany

Jürgen Eckert

IFW Dresden, Institut für Komplexe Materialien, Postfach 27 01 16, D-01171 Dresden, Germany

(Received 17 April 2007; accepted 24 April 2007; published online 15 May 2007)

Instead of applying severe plastic deformation, high-temperature heat treatment or high pressure, grain refinement and high-temperature phase separation induced by deformation in single-phase body-centered-cubic (bcc) coarse-grained Co–Fe alloys have been achieved by simple room-temperature compression. The alloys exhibit large plasticity over 140% without fracture. Phase separation from the bcc phase to nanoscale face-centered-cubic Fe and Co phases, which generally occurs at high temperature above ~ 1150 K, is formed in the deformed samples. The possible mechanisms are shear deformation and deformation-enhanced atomic diffusion rather than the temperature rise during deformation. © 2007 American Institute of Physics.

[DOI: 10.1063/1.2740476]

Plastic deformation is one of the popular solid-state processing methods to modify the microstructure and to improve both the physical and mechanical properties of engineering materials. For example, severe plastic deformation methods, including equal channel angular pressing (ECAP) and high-pressure torsion, have been widely used to produce bulk ultrafine- and/or nanoscale-grained metals and alloys.^{1–4} Compared with the coarse-grained starting materials, the deformation-induced fine-scale bulk materials exhibit excellent mechanical properties combining the high strength and large ductility owing to grain refinement by severe plastic deformation.^{2,3} However, the mechanism of the deformation-induced grain refinement to the ultrafine or nanoscale level is strongly related to the crystal structure of the investigated metallic materials.¹ On the other side, it has been reported that plastic deformation can induce phase transformations (such as nanocrystallization in metallic glasses,^{5,6} twinning, and martensitic transformation⁷).

Cobalt-iron alloys are ideally suited for industrial applications where high flux is required.^{8,9} However, the primary limitation of these alloys at present is not their high-temperature magnetic capability but their poor mechanical properties. It is well known that at room temperature the Co–Fe alloys are quite brittle when ordered and less brittle when disordered; a change accompanied by a transition from largely intergranular fracture to transgranular cleavage,¹⁰ which makes them unsuitable for industrial applications. Therefore, intensive research and development efforts over the years have resulted in a significant improvement of duc-

tility by microalloying (such as V) and a better understanding of the mechanical behavior and the phase transformations in Co–Fe alloys.^{8,9,11–14} Particularly, the order-disorder transition^{15–17} and the phase transitions from low-temperature body-centered-cubic (bcc) (α -Fe) to high-temperature face-centered-cubic (fcc) (γ -Fe + α -Co) (Refs. 16 and 18) or hexagonal-close-packed (hcp) (ϵ -Fe) (Ref. 19) structures in the Co–Fe base alloys have attracted considerable attention. In general, the order-disorder and bcc-fcc phase transitions have been investigated either by high pressure or by high-temperature heat treatment.^{15–19}

In this letter, we report on grain refinement and high-temperature phase separation induced by deformation in single bcc Co–Fe alloys obtained upon simple conventional room-temperature uniaxial compression, instead of applying severe plastic deformation, high-temperature heat treatment, or high pressure. The possible mechanisms for the deformation-induced grain refinement and phase separation into high-temperature phases at room temperature will be discussed.

The Co– x Fe ($x=25$ and 35 wt. %) alloys were prepared by arc melting a mixture of pure elements (99.9 wt. %) under a Ti-gettered argon atmosphere. The mechanical properties were evaluated under uniaxial compressive testing at room temperature. For this purpose, cylindrical specimens with 6 mm diameter and 9–12 mm length were cut from the arc-melted alloys and tested in an Instron 8562 testing machine at a strain rate of $1.2 \times 10^{-4} \text{ s}^{-1}$. Both loading surfaces were carefully polished to be parallel to an accuracy of less than 10 μm prior to compressive testing. The structural features before and after compression were examined by x-ray diffraction (XRD) using a Philips PW 1050 diffractometer

^{a)} Author to whom correspondence should be addressed; electronic mail: lczhangimr@gmail.com and l.zhang@ifw-dresden.de

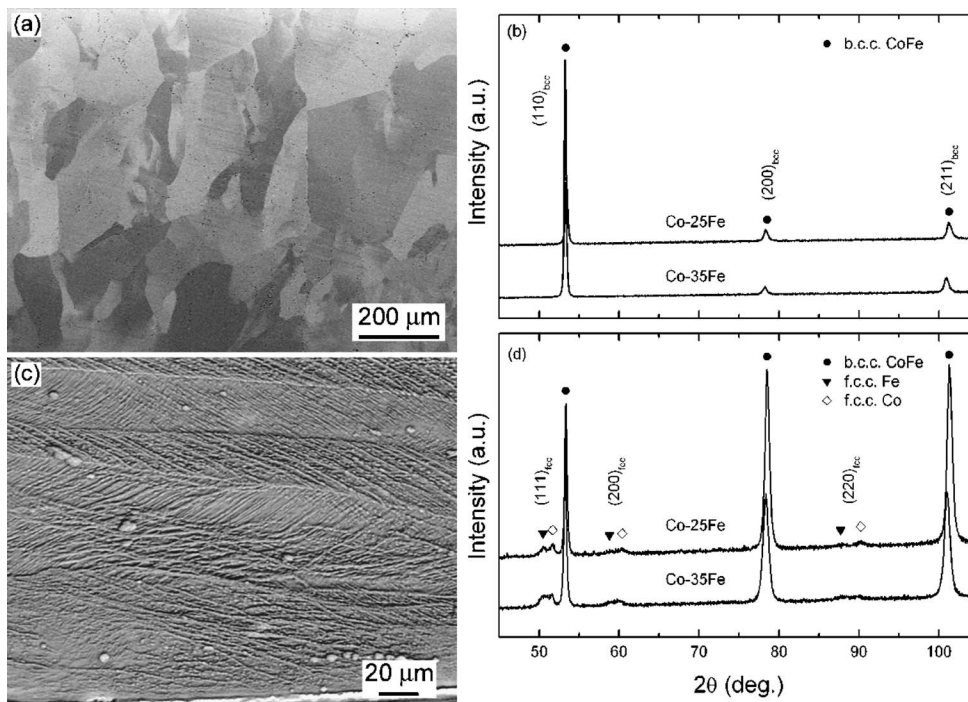


FIG. 1. SEM microstructure of the Co-25Fe alloy (a) before and (c) after deformation and XRD patterns of the Co-Fe alloys (b) before and (d) after deformation.

with monochromated Co $K\alpha$ radiation, JEOL JSM 6400 scanning electron microscopy (SEM), and Philips CM 20 transmission electron microscopy (TEM) coupled with energy-dispersive x-ray (EDX) analysis.

SEM analysis [Fig. 1(a)] of the arc-melted Co-25Fe alloys reveals a coarse-grained microstructure with a grain size in the range of 200–500 μm . The XRD patterns [Fig. 1(b)] show that both alloys consist of a single bcc CoFe phase. The lattice parameters of the CoFe phase, a_{CoFe} , are 0.2841 and 0.2848 nm for the Co-25Fe and Co-35Fe alloys, respectively. These values are consistent with the suggested lattice parameters equation for bcc Co-Fe.⁸

Figure 2 shows the uniaxial compressive true stress-strain curves at room temperature for the single-phase bcc Co-Fe alloys. Both alloys exhibit a similar deformation behavior: low yield strength ($\sigma_{0.2}$) (~ 355 and ~ 270 MPa for Co-25Fe and Co-35Fe alloys, respectively) and remarkable strain hardening from yielding up to the ultimate strength (~ 820 and ~ 1200 MPa) with a plastic strain (ϵ_p) exceeding 140%, without any loss of strength or fracture. The deformed

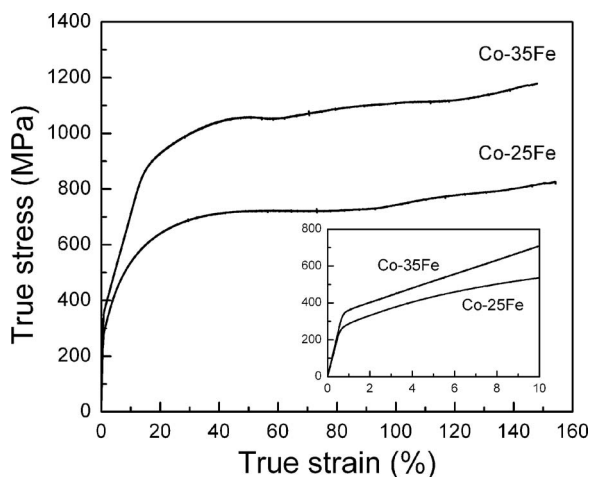


FIG. 2. Uniaxial compressive true stress-strain curves at room temperature for the single-phase bcc Co-Fe alloys.

samples display a drum shape. Elongated grains and a high density of wavy slip bands can be found in the longitudinal cross section of the deformed alloys [Fig. 1(c)]. These complex stress and complicated straining patterns will promote grain refinement and in turn enhance the plasticity of the alloys.²⁰ The XRD patterns of the deformed alloys [Fig. 1(d)] indicate that phase separation from a single low-temperature bcc phase to high-temperature fcc Fe and fcc Co has occurred upon compression at room temperature. The lattice parameters of the deformed bcc phase are 0.2840 and 0.2846 nm for the deformed Co-25Fe and Co-35Fe alloys, respectively. These values are somewhat smaller than those of the as-prepared alloys. The lattice distortion was estimated using the well-known Williamson-Hall method for the deformed bcc phase in the Co-25Fe and Co-35Fe alloys to be 0.20% and 0.29%, respectively. The grain size of the precipitated fcc phases is estimated to be less than 10 nm. The lattice parameters of the fcc Fe ($a_0=0.3659$ nm) and fcc Co ($a_0=0.3554$ nm) are 0.3660 and 0.3555 nm in the Co-25Fe alloys, and 0.3658 and 0.3559 nm in the Co-35Fe alloys, respectively. These means that deformation induces phase separation into pure fcc Fe and fcc Co upon room-temperature compression.

TEM observation [Fig. 3(a)] illustrates that a filamentary structure has formed after deformation, where the filamentary boundaries are indicated by arrows. The degree of deformation of the bcc filaments is inhomogeneous and increases from the sample surface towards the center (i.e., from the edge to the center in the TEM micrograph): one can find less, severely, and most severely deformed zones. Elongated filaments are located at the edge, while pronounced refined particles with a grain size in the range of 80–200 nm are visible at the severely deformed zones. Selected-area electron diffraction (SAED) patterns [Figs. 3(b) and 3(c)] and EDX analysis prove that the filaments and the refined particles are bcc phases. It is interesting to note that nanoscale high-temperature fcc Fe and fcc Co phases, as proved by SAED pattern [Fig. 3(d)] as well as by XRD [Fig. 1(b)], are

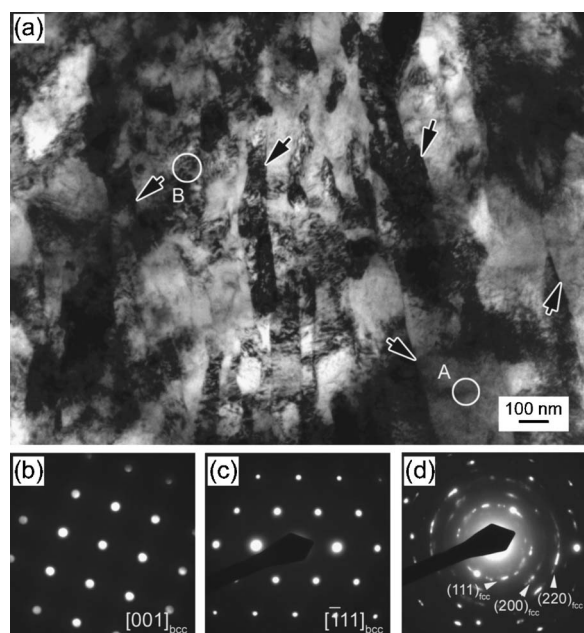


FIG. 3. TEM micrographs of the deformed Co–25Fe alloy: (a) bright-field image, corresponding selected-area electron diffraction patterns along (b) $[001]_{\text{bcc}}$ and (c) $[\bar{1}11]_{\text{bcc}}$ axes for the deformed bcc particle A and (d) for the phase separation zone B showing the deformation-induced phase separation into high-temperature phase at room temperature.

observed at the boundaries of fine bcc particles. Therefore, the deformed alloys show a bimodal microstructure consisting of multiscale grains, which is believed to greatly contribute to the large plasticity of the Co–Fe alloys.²⁰ Meanwhile, deformation-induced phase transition into nanoscale fcc phases with more slip systems will also enhance their plasticity.⁷

The bcc–fcc phase transition typically occurs at high temperature (~ 1150 K), dependent on compositions according to the Co–Fe binary phase diagram.²¹ However, this high-temperature phase separation has been achieved under the present conventional compressive testing conditions at room temperature. At first glance, the high-temperature phase separation could be postulated to be related to a deformation-induced temperature rise. Experimental measurements of the temperature rise upon bend testing based on a fusible tin coating²² showed that there can be a remarkable local temperature rise of thousands of degrees for a few nanoseconds. Such a high local temperature rise may induce high-temperature phase transitions (in our case, phase separation). It has been reported that the high-temperature phase separation on the surface of the Fe–50Co alloy can be detected by heat treatment at 1273 K for 4 h, followed by water quenching.¹⁶ Therefore, owing to the ultrafast heating and the short holding time at the assumptive high temperature induced by plastic deformation, atomic diffusion will be kinetically limited in the phase transition. In addition, the fcc phase will transform back to the bcc phase under slow cooling in air. This is quite similar to the deformation-induced nanocrystallization in amorphous alloys,^{5,23} which was argued not to directly result just from the deformation-induced temperature rise. It is known that the bcc \leftrightarrow fcc phase transition in Co–Fe alloys is diffusion controlled.²⁴ The formation of the filamentary structure in the deformed Co–Fe alloys [Fig. 3(a)] is analogous to the scenario in ball milling^{25,26} and ECAP,⁴ where shear deformation and deformation-enhanced

atomic diffusion under plastic deformation lead to grain refinement and/or phase transformation. In fact, as illustrated by the TEM observation [Fig. 3(a)], the deformation degree of the bcc filaments is inhomogeneous and increases from the sample surface towards the center. Pronounced grain refinement locates at the severely deformed zones, while high-temperature phase separation appears at the most severely deformed zones. In contrast, dislocations and elongated bcc filaments are found in the less deformed zones. These phenomena are quite similar to the scenario in the case of different milling times during ball milling and different passes for ECAP.^{4,25,26} Further detailed investigations concerning the effects/competition of ordering, clustering, and phase separation in this alloy system are underway and will be published in a forthcoming paper.

In summary, we have achieved pronounced grain refinement and nanoscale phase separation into high-temperature phase upon the conventional compression of initially coarse-grained Co–Fe alloys at room temperature. The observed phenomena are a consequence of the shear deformation and dramatic deformation-enhanced atomic diffusion during deformation. The alloys exhibit large plasticity over 140% without fracture, which is contributed to the deformation-induced nanostructuring and bimodal microstructure.

The authors thank H. Ehrenberg and T. G. Woodcock for stimulating discussions and M. Frey, H. J. Klauß, and S. Kuszinski for technical assistances. Two of the authors (L.C.Z. and M.C.) are very grateful for the financial support of the Alexander von Humboldt Foundation.

- ¹R. Z. Valiev and T. G. Langdon, *Prog. Mater. Sci.* **51**, 881 (2006).
- ²D. Jia, Y. M. Wang, K. T. Ramesh, E. Ma, Y. T. Zhu, and R. Z. Valiev, *Appl. Phys. Lett.* **79**, 611 (2001).
- ³X. Z. Liao, A. R. Kilmametov, R. Z. Valiev, H. S. Gao, X. D. Li, A. K. Mukherjee, J. F. Bingert, and Y. T. Zhu, *Appl. Phys. Lett.* **88**, 021909 (2006).
- ⁴A. Mishra, B. K. Kad, F. Gregori, and M. A. Meyers, *Acta Mater.* **55**, 13 (2007).
- ⁵J. J. Kim, Y. Choi, S. Suresh, and A. S. Argon, *Science* **295**, 654 (2002).
- ⁶L. C. Zhang, J. Xu, and E. Ma, *Mater. Sci. Eng., A* **434**, 280 (2006).
- ⁷W. Xu, K. B. Kim, J. Das, M. Calin, B. Rellinghaus, and J. Eckert, *Appl. Phys. Lett.* **89**, 031906 (2006).
- ⁸T. Sourmail, *Prog. Mater. Sci.* **50**, 816 (2005).
- ⁹R. S. Sundar and S. C. Deevi, *Int. Mater. Rev.* **50**, 157 (2005).
- ¹⁰T. L. Johnston, R. G. Davies, and N. S. Stoloff, *Philos. Mag.* **12**, 305 (1965).
- ¹¹A. Duckham, D. Z. Zhang, D. Liang, V. Luzin, R. C. Cammarata, R. L. Leheny, C. L. Chien, and T. P. Weihs, *Acta Mater.* **51**, 4083 (2003).
- ¹²L. Zhao and I. Baker, *Acta Metall. Mater.* **42**, 1953 (1994).
- ¹³C. D. Pitt and R. D. Rawlings, *Met. Sci.* **17**, 261 (1983).
- ¹⁴E. P. George, A. N. Gubbi, I. Baker, and L. Robertson, *Mater. Sci. Eng., A* **329–331**, 325 (2002).
- ¹⁵J. A. Oyedele and M. F. Collins, *Phys. Rev. B* **16**, 3208 (1977).
- ¹⁶Y. Ustinovshnikov and S. Tresheva, *Mater. Sci. Eng., A* **248**, 238 (1998).
- ¹⁷T. Sourmail, *Scr. Mater.* **52**, 1347 (2005).
- ¹⁸M. S. Seehra and P. Silinsky, *Phys. Rev. B* **13**, 5183 (1976).
- ¹⁹D. Papantonis and W. A. Bassett, *J. Appl. Phys.* **48**, 3374 (1977).
- ²⁰Y. M. Wang, M. W. Chen, F. H. Zhou, and E. Ma, *Nature (London)* **419**, 912 (2002).
- ²¹T. B. Massalski, H. Okamoto, P. R. Subramanian, and L. Kacprzak, *Binary Alloy Phase Diagrams* (ASM, Materials Park, OH, 1996), Vol. 2, p. 1186.
- ²²J. J. Lewandowski and A. L. Greer, *Nat. Mater.* **5**, 15 (2006).
- ²³L. C. Zhang, K. B. Kim, P. Yu, W. Y. Zhang, U. Kunz, and J. Eckert, *J. Alloys Compd.* **428**, 157 (2007).
- ²⁴S. G. Fishman, D. Gupta, and D. S. Lieberman, *Phys. Rev. B* **2**, 1451 (1970).
- ²⁵M. Seidel, J. Eckert, I. Bächer, M. Reibold, and L. Schultz, *Acta Mater.* **48**, 3657 (2000).
- ²⁶C. C. Koch, *Mater. Sci. Forum* **88–90**, 243 (1992).